N77-18101

GENERAL AVIATION CRASH SAFETY PROGRAM AT LANGLEY RESEARCH CENTER

Robert G. Thomson
NASA Langley Research Center

SUMMARY

The purpose of the Langley Research Center crash safety program is to support development of the technology to define and demonstrate new structural concepts for improved crash safety and occupant survivability in general aviation aircraft. The program involves three basic areas of research: full-scale crash simulation testing, nonlinear structural analyses necessary to predict failure modes and collapse mechanisms of the vehicle, and evaluation of energy absorption concepts for specific component design. Both analytical and experimental methods are being used to develop expertise in these areas. Analyses include both simplified procedures for estimating energy absorption capabilities and more complex computer programs for analysis of general airframe response. Under the crash safety program, these analyses will be developed to provide the designer with methods for predicting accelerations, load, and displacement histories of collapsing structures. Full-scale tests of typical structures as well as tests on structural components are being used to verify the analyses and to demonstrate improved design concepts.

INTRODUCTION

Technology for predicting aircraft dynamic response under crash loads and occupant behavior during impact is being developed by Langley Research Center (LaRC) in a joint NASA/FAA crashworthiness program. Part of the analytical and experimental program includes evaluating airframe, seat, and restraint-system concepts for mitigating crash loads imposed on occupants of general aviation aircraft. The methods used and concepts developed from these ongoing efforts will make feasible future aircraft designs that will enhance the degree of survivability under a crash condition with minimum weight and cost penalties. The total program with its goal of improved occupant survivability following an airplane accident is shown in figure 1. NASA's responsibility in this joint program is shown as shaded boxes, the FAA's role as unshaded boxes, and joint efforts as crosshatched boxes.

Crashworthiness design technology is divided into three areas: environmental, airframe design, and component design. The environmental factors consist of acquiring and evaluating actual field crash data and defining a crash envelope within which the impact parameters allow tolerable acceleration levels.

Airframe design has a twofold objective: to assess and apply current, on-the-shelf, analytical methods to predict structural collapse; and to develop and validate advanced analytical techniques. NASA's primary role

in the joint program is the development of advanced analytical techniques. Full-scale tests will be used to verify the analytical predictions, as well as to demonstrate improved crashworthy design concepts. A facility for free-flight crash testing of full-scale aircraft structures and structural components has been developed at LaRC. Airframe design also includes evaluation of novel crashworthy design concepts and their effect on structural crashworthiness.

Component design consists of exploring the development of new and innovative energy-absorbing concepts to improve performance of seats and occupant restraint systems as well as the design of nonlethal cabin interiors.

LaRC CRASH SAFETY PROGRAM

The responsibilities of LaRC in the airframe design technology portion of the joint program (see fig. 2) can be divided into three program elements: full-scale crash simulation testing, nonlinear crash impact analysis, and crashworthy design concepts.

Full-Scale Crash Simulation Testing

The full-scale crash simulation testing is being done at LaRC in the Langley impact dynamics research facility (ref. 1) shown in figure 3. This facility is the former Langley lunar landing research facility that has been modified for free-flight crash testing of full-scale aircraft structures and structural components under highly controlled test conditions. The test vehicles are suspended from the gantry and then swung pendulum fashion and released to simulate free-flight crash conditions at impact.

The facility's basic gantry structure is 73 m (240 ft) high and 122 m (400 ft) long supported by three sets of inclined legs spread 81 m (267 ft) apart at the ground and 20 m (67 ft) apart at the 66-m (218-ft) level. A movable bridge spans the top and traverses the length of the gantry.

Test method.- The method for crash testing the aircraft is shown pictorially in figure 4. The aircraft is suspended from the top of the gantry by two swing cables and is drawn back above the impact surface by a pullback cable. An umbilical cable used for data acquisition is also suspended from the top of the gantry and connects to the top of the aircraft. The test sequence is initiated when the aircraft is released from the pullback cable. The aircraft swings pendulum style into the impact surface. The swing cables are separated from the aircraft by pyrotechnics just prior to impact, freeing the aircraft from restraint. The umbilical cable remains attached to the aircraft for data acquisition, but it also separates by pyrotechnics before it becomes taut during skid out. Since the separation point is held relatively fixed near the impact surface, the length of the swing cables is used to adjust the flight-path angle from 0° to 60°. The height of the aircraft above the impact surface at release determines the impact velocity and can be varied to give impact velocities from 0 to 26.8 m/s (60 mph). It is important that, in the suspended position, the

force vectors of the swing cables and pullback cables act at 90° to each other and pass through the center of gravity of the aircraft. This is necessary to control aircraft pitch reaction during the swing phase. The movable bridge allows the pullback point to be positioned along the gantry to insure this force relation for various pullback heights and swing-cable lengths. The pitching velocity of the aircraft at swing-cable separation continues to change the pitch attitude of the aircraft during the free-flight phase of the test. In the 10 tests conducted to date, the pitch angle change due to this condition has never been greater than 1.75°.

A typical aircraft suspension system which is designed specifically for the aircraft configuration being tested is shown in figure 5. The swing cables attach to hard points in the main wing spar of the aircraft so that a line connecting the two hard points (dashed line in figure) passes directly through the aircraft center of gravity. The pullback cable attaches to these same hard points; thus, its force reaction also passes through the center of gravity. Two sets of pitch cables are attached to the swing cables 3 m (10 ft) above the hard points in the wings and to hard points in the fuselage fore and aft of the aircraft center of gravity. Adjustments in roll angle to about 30° can be made, without sacrificing control, by varying the length of the swing and pitch cables. Adjustments in yaw angle to about 15° can be made by varying the length of the cables in the pullback harness and the pitch cables. Adjustments in pitch to about 45° can be made by varying the length of the pitch cables in the fore and aft directions. Larger changes in pitch, yaw, and roll require redesign and/or relocation of the hard points in the aircraft. For other aircraft configurations, the hard points must be properly located and a new suspension system must be designed to maintain the swing and pullback cables at 90° to each other with their force vectors passing through the aircraft center of gravity.

Instrumentation.- Data gathering from the full-scale crash test of an aircraft is accomplished with extensive photographic coverage, both interior and exterior to the fuselage, utilizing low-, medium-, and high-rate cameras and with onboard strain gages and accelerometers. The piezoelectric accelerometers (range of 250g and 2 to 5000 Hz) are the primary data-generating instruments. A typical accelerometer layout for a test specimen experiencing zero yaw at impact is shown in figure 6. Circles indicate instruments positioned to measure accelerations normal to the fuselage's horizontal plane. Diamonds represent instruments positioned to measure accelerations both in the normal and longitudinal directions as shown in the figure. The side-view schematic also shows two dummies onboard the test specimen. There have been from one to four anthropomorphic dummies (National Highway Traffic Safety Administration Hybrid II) onboard all full-scale aircraft tests conducted to date at LaRC. Shown in figure 7 is a schematic of a typical onboard camera and restraint-system arrangement. The forward camera is located in the radio compartment in the instrument panel, the rear camera on a rear instrument shelf, and the two side cameras are cantilevered off the fuselage. These cameras are shock resistant and are mounted in a cantilever fashion. There are approximately 15 exterior cameras used during a test. The location and framing rate of these cameras are discussed in reference 1. The restraint-system arrangement and type of restraint used vary from test to test.

Tests conducted.- Full-scale crash testing of aircraft and aircraft components is being conducted at LaRC to determine a set of structural design crash parameters for which the cabin area maintains its structural integrity to the degree that it supports a livable volume throughout the crash sequence. These structural crash parameters will be supplemented by FAA field crash data to form a basis for a rational crash design envelope. In addition, the experimental crash test data will be used to ascertain the validity of analytical predictions and to test the performance of improved structural and seat concepts for crashworthiness. The initial stages of the crash test program, from February 1974 to June 1976, have been conducted using 10 twin-engine light aircraft impacting into a concrete surface.

A summary of the impact parameters associated with these 10 tests is shown in figure 8 by the shaded boxes. The flight-path angle was maintained at -15° except for two tests. These two tests had flight-path angles of -30° and -45°. The flight-path velocity has been held constant at 26.8 m/s (60 mph) except for one test at 13.4 m/s (30 mph). Two tests were performed with landing gear extended and are indicated by an asterisk. Positive angles of attack of 15° and 30° were introduced in two tests at -15° flight-path angle. In addition, two tests were conducted with negative roll angles of 30° and 15°.

Future full-scale aircraft tests, shown in figure 8 by unshaded boxes, will include twin-engine aircraft at lower impact flight-path angles but higher impact velocities (aircraft's swing velocity will be augmented with wing-mounted rocket motors). In addition, three high- and three low-wing, single-engine aircraft crash tests are planned, as well as stripped airframe tests on field terrain simulated by dirt. The matrix of full-scale crash testing is by no means complete and does not consider such secondary effects as aircraft sliding, overturning, cartwheeling, or tree and obstacle impact. However, the proposed crash tests should generate enough meaningful crash data to define single- and twin-engine structural crash test envelopes.

NASA full-scale crash test data.- Experimental acceleration time history data and structural damage assessment, generated from each of NASA's full-scale crash tests, are being analyzed for publication. The analyses consider the effects of varying one of the impact parameters only, such as, flight-path velocity, flight-path angle, angle of attack, or roll. A representative sample of the type of data to be reported is presented herein for 1 of the 10 tests shown in figure 8 (nominal test conditions of 26.8 m/s (60 mph) flight-path velocity, -15° flight-path angle, zero angle of attack, and zero roll and yaw).

Figure 9 is a sequence of photographs taken with a 20-frame-per-second camera during the second crash test. Time between frames is 0.05 second. The sequence clearly shows the free-flight condition of the test aircraft prior to impact at 26.8 m/s (60 mph) and a pitch angle of -12°. The structural damage to the fuselage occurs during two impacts: primary impact when the nose initially impacts the ground surface (third frame) and secondary impact when the cabin slams down onto the ground surface because of fuselage rotation (fifth frame). This secondary impact produces the most severe normal accelerations in the cabin area. For this particular test, structural damage was moderate with the cabin maintaining its livable volume. Rivet shear occurred

in the cabin along lines of overlapping skin sheet metal and interior stiffening structure. Breaks due to this rivet shear appeared in the roof at the main spar frame, along the window ledges, and in the vicinity of the door. Upon impact, the forward floor beams and nose wheel well rotated upward causing buckling of the entire nose, fire wall, and floor beams in the cockpit. The combination of downward momentum of the wings and the impact of the main spar with the ground produced twisting of the main spar and loss of wing dihedral angle. In addition, the cabin floor experienced upward heaving of the floor beams causing outboard seat rotation. Glass breakage was confined to the pilot's windscreen and side window.

Four representative sets of acceleration time histories, normal to the longitudinal axis, recorded during this full-scale crash test are presented in figures 10, 11, 12, and 13. At the top of each figure there is a side-view schematic locating the accelerometers (diamond symbols) and the four anthropomorphic dummies (pilot, copilot, and two passengers) of interest. Figures 10 and 11 are typical acceleration time histories while figures 12 and 13 are acceleration time histories with timed events from photographic data superimposed on the acceleration traces.

Figure 10 presents acceleration traces at two different locations normal to the floor beam of the fuselage. The first accelerometer is located at the initial point of impact, first fuselage frame. Acceleration trace (2) is aft of the first passenger and is not affected by the primary impact but by the secondary impact when the cabin compartment slams onto the contact surface. The fuselage directly below point (2) contacts the ground 0.09 second after initial ground contact (fifth frame of fig. 9). For the nose location at the first fuselage frame (trace (1)) during the first 0.1 second after impact, the aircraft exhibits high amplitude oscillatory behavior caused by initial impact (120g negative acceleration), then rebound (42g positive acceleration) followed by another impact (40g negative acceleration) which is canceled by the action of the adjacent structure as it continues along the flight path. Although the secondary impact produces the most severe normal accelerations in the cabin area, the magnitudes of these accelerations (22g negative and 50g positive) are still substantially lower than those of the nose (impact point) accelerations and occur between 0.1 and 0.2 second after primary impact.

Figure 11 presents time history of the average of four accelerometers located normal to the base of the first passenger seat (behind the pilot) and the normal pelvic acceleration time history of the anthropomorphic dummy. The first passenger (79.3 kg (175 lb)) was seated in a standard passenger seat and was restrained by a five-point restraint system - lap belt, crotch belt, and two shoulder harnesses. The average seat input (at the base of the seat) peaks at about 0.08 second after initial impact. There is some similarity between the average acceleration trace of the seat base (3) and the first passenger pelvic trace (4) if one considers that there is a time lag of 0.02 second between the traces during which the seat cushion and dummy compress. However, little energy is dissipated by the seat structure as is evident in the small difference in maximum acceleration peaks between the seat base (3) (54g positive) and the dummy's pelvis (4) (50g negative).

In figure 12, six normal acceleration time history traces are presented with timed events from photographic data superimposed on the traces for correlation and interpretation. The six accelerometers are spaced along the floor beam of the aircraft from the first fuselage frame to the rear of the first passenger seat (see side- and top-view insert). The response of initial ground contact is felt immediately at the first frame (trace (1)) and is seen to progress rearward to the fire wall (trace (3)) with diminishing intensity and with a slight time lag associated with the rearward progression of the contact surface. Main spar ground contact (0.05 second) produces a positive acceleration or downward force in the nose of the aircraft and signals the initiation of cabin compartment excitation. The intensity of the acceleration peaks in the cabin compartment is maximum in the vicinity of the main spar and diminishes progressively from that point rearward. The secondary impact due to downward fuselage rotation produces a negative acceleration peak (or upward force) in the cabin compartment (60g on trace (4), 40g on trace (5)). The loss of wing dihedral angle and wing ground contact have little overall effect on the fuselage response except for the main spar twisting. The rivet shear failure of the fuselage in the roof at the main spar, 0.178 second after impact, concludes further significant crash effects felt in the aircraft structure.

Acceleration time history traces of the anthropomorphic dummy at the first passenger location and of the seat at the base of each leg are shown in figure 13 superimposed with timed events from photographic data. Initial ground contact, indicated by zero time in figure 13, is not felt appreciably by the first passenger. The first passenger begins downward and forward motion 0.06 second after impact at precisely the time that the front and rear legs of the seat first begin to record large localized forces. The seat then begins to rotate outboard (0.069 second). The shapes of the pulses of the two front seat legs are nearly identical as are the shapes of the pulses of the two rear seat legs. The primary pulse into each leg (the time interval between 0.07 to 0.09 second) has practically the same period but much lower amplitude in the rear legs of the seat. This primary pulse is exhibited in the pelvic region (trace (3)) of the dummy 0.025 second later. For determining a single acceleration pulse shape for seat evaluation, it appears that the simple averaging of the inputs at each leg attachment point (fig. 11) yields a satisfactory representation. Comparison of aisle leg to window leg accelerations indicates that the aisle leg negative acceleration peaks during seat rotation are higher than the corresponding window leg peaks. This difference is due to the aisle floor structure impacting first and causing outboard seat rotation. At the end of the outboard seat rotation a positive (downward) normal acceleration peak (70g and 63g) occurs in both rear seat legs as the dummy moves rearward in the seat, and at the end of dummy forward pitching, a large negative longitudinal acceleration (70g on trace (2)) occurs because of tightening of the restraint system. (The normal and longitudinal dummy acceleration traces are taken relative to a local dummy coordinate system perpendicular and parallel to the dummy's spine.) Cabin lateral expansion ends at 0.146 second, which marks the end of significant seat and dummy response. The cabin's lateral elastic recovery occurs by 0.306 second.

Nonlinear Crash Impact Analysis

The objective of the analytical efforts at LaRC is to develop the capability to predict the nonlinear geometric and material behavior of sheet-stringer aircraft structures subject to large deformations and to demonstrate this capability by determining the plastic buckling and collapse response of such structures to impulsive loadings. Two specific finite-element computer programs are being developed with attention focused on modeling concepts applicable to large plastic deformations of realistic aircraft structural components. These two programs are discussed in the following sections. Other current computer programs available for crashworthy analysis are reviewed in reference 2. This review deals primarily with modeling concepts and the relative capabilities and limitations of nonlinear computer programs for application to large plastic deformations of realistic vehicle structures.

PLANS.- For several years LaRC has been developing a rather sophisticated plastic analysis computer program (Plastic and Large Deflection Analysis of Nonlinear Structures) which includes geometric as well as material nonlinearities (refs. 3 and 4). This computer program for static finite-element analysis is capable of treating problems which include bending and membrane stresses, thick and thin axisymmetric bodies, general three-dimensional bodies, and laminated composites. The solution procedure embodies the initial strain concept which reduces the nonlinear material analysis to the analysis of an elastic body of identical shape and boundary conditions, but with an additional set of applied "effective plastic loads." The advantage of this solution technique is that it does not require modification of the element stiffness matrix at each incremental load step.

ACTION.- A nonlinear dynamic finite-element computer program (Analyzer of Crash Transients in Inelastic or Nonlinear Response (CRASH in ref. 5)) is being extended at LaRC to more realistic aircraft sheet-stringer structures. Membrane elements have been added to the initial truss and frame simulation capability to predict the transient response of frames with and without sheet coverings. This new computer program uses direct energy minimization to obtain solutions rather than the usual direct stiffness method which requires modifications of the initial stiffness matrix for plastic material behavior.

Analytical and experimental results.- These computer programs are currently being evaluated by comparison with experimental results on some simplified structures. These structures are shown in figure 14 in the order of increasing complexity: an axial compression of a circular cylinder, a tubular structure composed of 12 elements with symmetric cross sections joined at common rigid joints, an angular frame composed of asymmetric angles and bulkheads with nodal eccentricities at the rigid joints, and the same angular frame covered with sheet material. Static and dynamic analyses of these structures loaded into the large deflection plastic collapse regime are being conducted with PLANS and ACTION and are being compared with experimental data. Large deflection static analyses with corroborating experimental results, for the simplified structures shown in figure 14, are reported in reference 6.

Figure 15 is a photograph of the angular frame structure which measures 1.5 m (5 ft) in length with a base 1.3 m by 1 m (4.2 ft by 3.3 ft) tapering

to 0.61 m by 0.57 m (2 ft by 1.87 ft) at the tip. The frame is composed of rigid bulkheads connected longitudinally by 2.54 cm by 2.54 cm by 0.16 cm (1 in. by 1 in. by 0.0625 in.) angle. A T-beam made of two riveted 2.54 cm by 2.54 cm by 0.24 cm (1 in. by 1 in. by 0.094 in.) angles braces the rear bulkhead with a center T-beam of the same dimensions. Shown in figure 16 is a chronological sequence of computer deformation patterns for the angular frame loaded impulsively. The end (smallest) bulkhead of the angular frame was given an initial longitudinal velocity at time zero of 13.4 m/s (30 mph); the remainder of the frame was kept at rest.

Computer predictions of the subsequent deformation patterns of the angular frame obtained with the PLANS computer program are shown in figure 16 for various times (in milliseconds) after initial impact. The computer predictions indicate no appreciable collapse of the first bay of the angular frame for the 13.4 m/s (30 mph) loading. Plastic stresses and deformations are present, however, in the first bay. In igure 17 the frame is loaded impulsively (at the end bulkhead) with an initial velocity of 89.4 m/s (200 mph). The frame, under this loading condition, experiences collapse in the first bay in 0.70 millisecond. Corroboration of the analytical predictions with experimental data is to be accomplished by explosively loading the angular frame in a sequence of experimental tests with explosive sheet, detonated with fuse cord. A schematic and photograph of the test setup showing the angular frame positioned vertically with the loading on the end bulkhead are given in figure 18.

Crashworthy Design Concepts

The final area of research in the crash safety program is the development of crashworthy design concepts. The objective here is to develop structural concepts that improve the energy absorption characteristics of a structure either by modifying its structural assembly, changing the geometry of its elements, or adding specific energy absorption devices to help dissipate kinetic energy. Recent efforts in this research area at LaRC have been concentrated on the development of crashworthy aircraft seat and restraint systems. A user-oriented computer program called SOMLA (Seat Occupant Model-Light Aircraft), described in reference 7, is being used to study seat and occupant response under crash loading conditions. The computer program is based on a three-dimensional occupant and seat model in which the occupant model consists of 11 rigid mass segments. The seat model is composed of beam and membrane elements with provision for simulating plastic behavior by the use of plastic hinges. (See fig. 19.) Verification efforts of SOMLA using LaRC full-scale crash test data have resulted in the incorporation of modifications to allow for more realistic simulation of seat leg loading and occupant/restraint-system interface.

A comparison of SOMLA's computer predictions with experimental data from an aircraft section drop test is presented in figure 20. The aircraft section is a 1.5 m (5 ft) longitudinal fuselage section of a twin-engine aircraft beginning directly behind the pilot and containing the first row of passengers. (See fig. 21.) The solid curves in figure 20 are experimental accelerations for an aisle seat leg, a window seat leg, and the pelvis of the first passenger

(behind the pilot). The first passenger is seated in a standard aircraft passenger seat. The dashed curve is the computer prediction of the pelvis response for the first passenger (50 percentile male anthropomorphic dummy). The peak magnitude and duration of the pelvis response show good correlation with the experimental data. However, the experimental data exhibit an initial negative (upward) acceleration which diminishes as the seat cushion compresses, followed by a second negative peak as the occupant is loaded by the seat frame. The failure of SOMLA to predict this response is due to the occupant being loaded through node points which are time invariant.

Two-dimensional computer graphics of SOMLA's seat, occupant, and restraint-system response for the aircraft section drop test are shown in figure 22. The computer graphics show the occupant compressing the seat cushion and the slacking (gapping) of the seat belt. No shoulder harness was simulated because of the vertical test condition and the immediate flexing of the upper portion of the aircraft section, artificially unloading the test dummies' shoulder harnesses, as shown in figure 21. Computer graphic displays, as illustrated in figure 22, aid in visually interpreting the combined motions of the seat, occupant, and restraint system during the crash sequence; they are also helpful in verifying modeling techniques and data input.

CONCLUDING REMARKS

Langley Research Center (LaRC) has initiated a crash safety program that will lead to the development of technology to define and demonstrate new structural concepts for improved crash safety and occupant survivability in general aviation aircraft. This technology will make possible the integration of crashworthy structural design concepts into general aviation design methods. The technology will include airframe, seat, and restraint-system concepts that will dissipate energy and properly restrain the occupants within the cabin interior. The current efforts at LaRC are focused on developing improved aircraft components needed for crash protection, and both improved seat and restraint systems are being considered as well as structural airframe modifications. The dynamic nonlinear behavior of these components is being analytically evaluated to determine tneir dynamic response and to verify design modifications in structural crushing efficiency. In particular, that portion of the aircraft which surrounds the cabin area is being studied to determine methods of effectively dissipating crushing loads from three different vector directions while maintaining cabin integrity. Seats and restraint systems with deceleration devices incorporated are being studied that will absorb energy, remain firmly attached to the cabin floor, and adequately restrain the occupant from impact with the cabin interior. Full-scale mockups of structural components are being used to verify and provide corroboration to the analytical design methods.

In the development of aircraft design criteria, a set of design crash parameters are to be determined from both FAA field data and LaRC structural crash test data. The structural crash test data will include controlled crashes at velocities comparable with the stall velocity of most general aviation aircraft. Close cooperation with other governmental agencies is being maintained to provide inputs for human tolerance criteria concerning the magnitude and

duration of deceleration levels and for realistic crash data on survivability. Development of reliable crashworthiness design methods and analytical techniques for effective crash protection of general aviation aircraft is the final goal of the LaRC crash safety program.

REFERENCES

1. Vaughan, Victor L., Jr.; and Alfaro-Bou, Emilio: Impact Dynamics Research Facility for Full-Scale Aircraft Crash Testing. NASA TN D-8179, 1976.

2. McIvor, Ivor K.: Modeling and Simulation as Applied to Vehicle Structures and Exteriors. Vehicle Safety Research Integration Symposium, Rep. No. DOT HS-820 306, U.S. Dep. Transp., May 1973, pp. 5-18.

3. Armen, H., Jr.; Pifko, A.; and Levine, H. S.: Finite Element Analysis of Structures in the Plastic Range. NASA CR-1649, 1971.

4. Pifko, A.; Levine, H. S.; Armen, H., Jr.; and Levy, A.: Plans - A Finite Element Program for Nonlinear Analysis of Structures. Paper 74-WA/PVP-6, American Soc. Mech. Eng., Nov. 1974.

5. Melosh, Robert J.: Car-Barrier Impact Response of a Computer Simulated Mustang. Rep. No. DOT-HS-091-1-125-A, U.S. Dep. Transp., Mar. 1972.

6. Alfaro-Bou, E.; Hayduk, R. J.; Thomson, R. G.; and Vaughan, V. L., Jr.: Simulation of Aircraft Crash and Its Validation. Aircraft Crashworthiness, Kenneth Saczalski, George T. Singley III, Walter D. Pilkey, and Ronald L. Huston, eds., Univ. Press of Virginia, c.1975, pp. 485-497.

7. Laananen, David H.: Development of a Scientific Basis for Analysis of Aircraft Seating Systems. Rep. No. FAA-RD-74-130, January 1975.

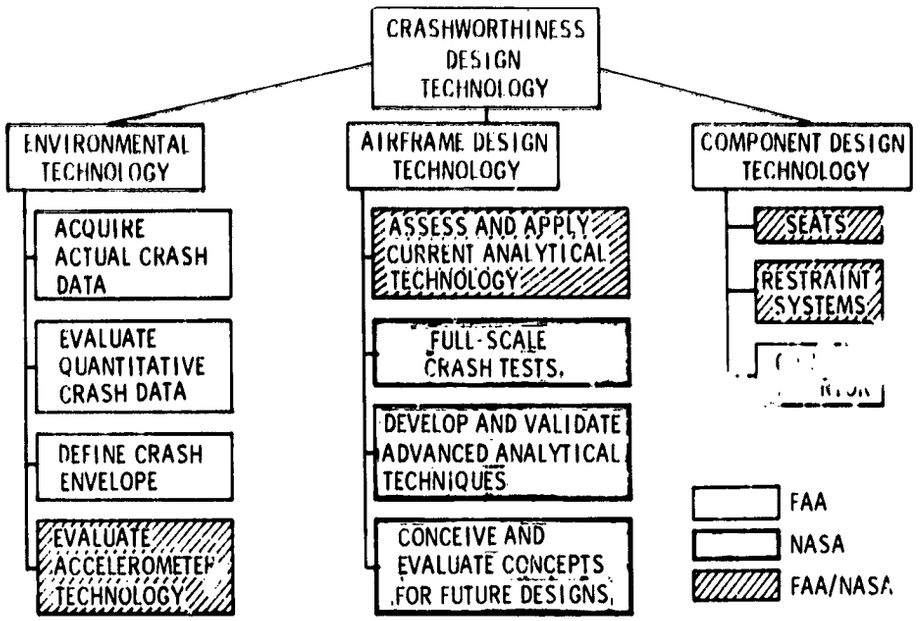

Figure 1.- Agency responsibilities in joint FAA/NASA general aviation crashworthiness program.

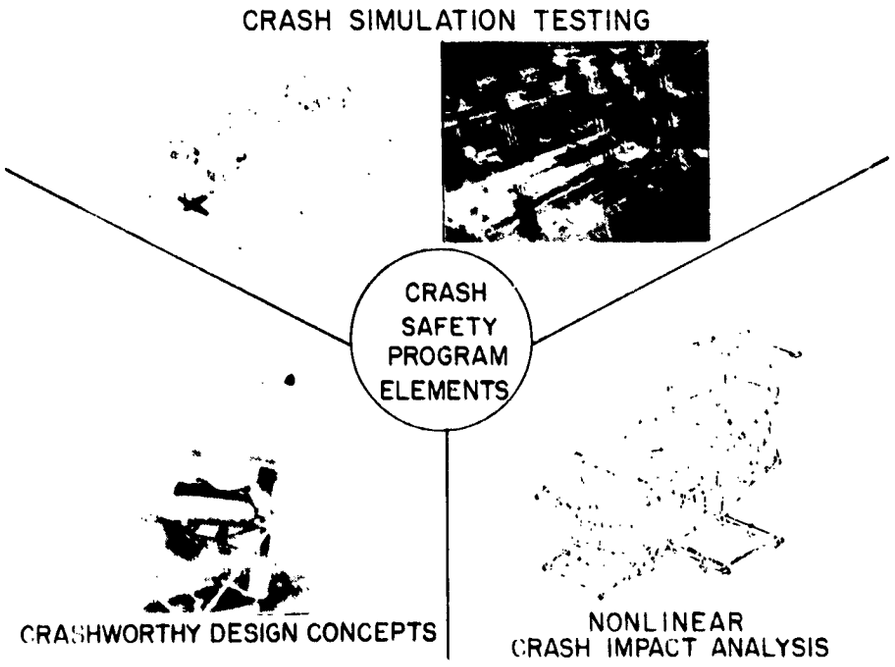

Figure 2.- Elements of LaRC crash safety program.

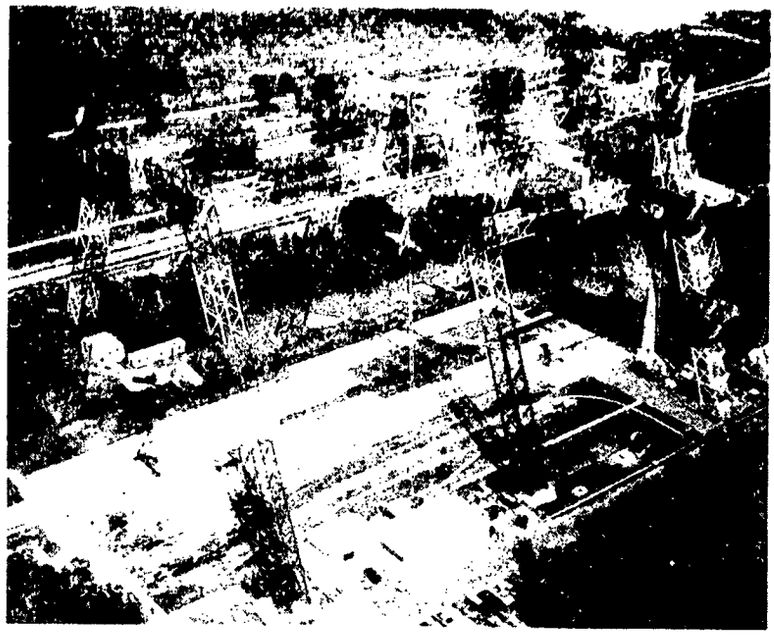

Figure 3.- Langley impact dynamics research facility.

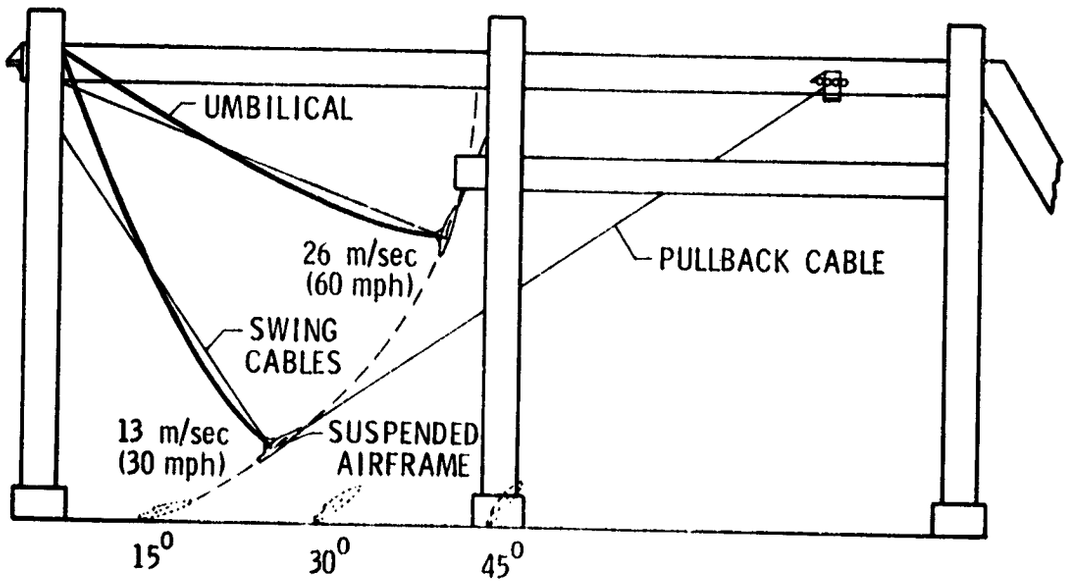

Figure 4.- Aircraft crash test method.

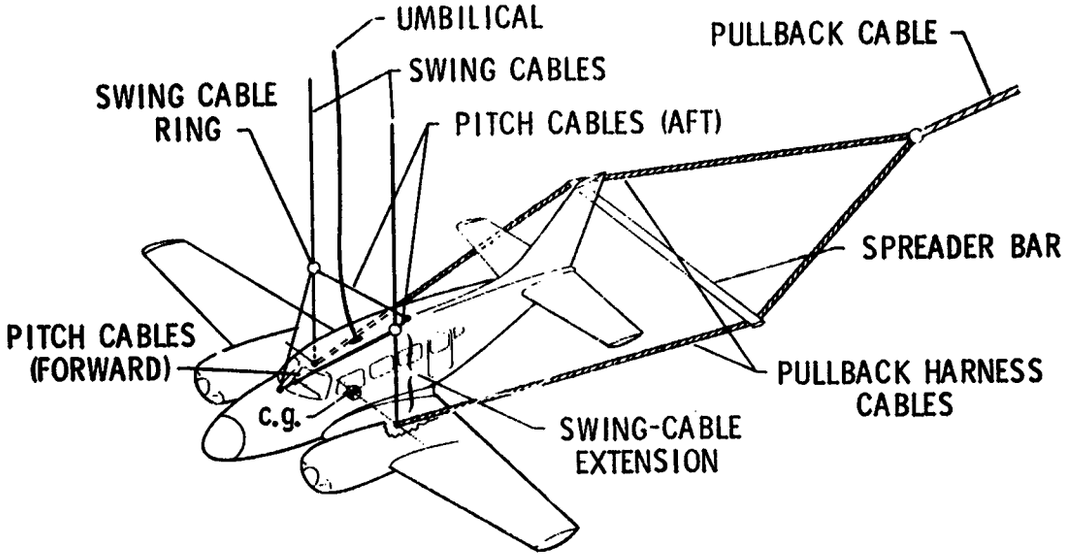

Figure 5.- Typical aircraft suspension system.

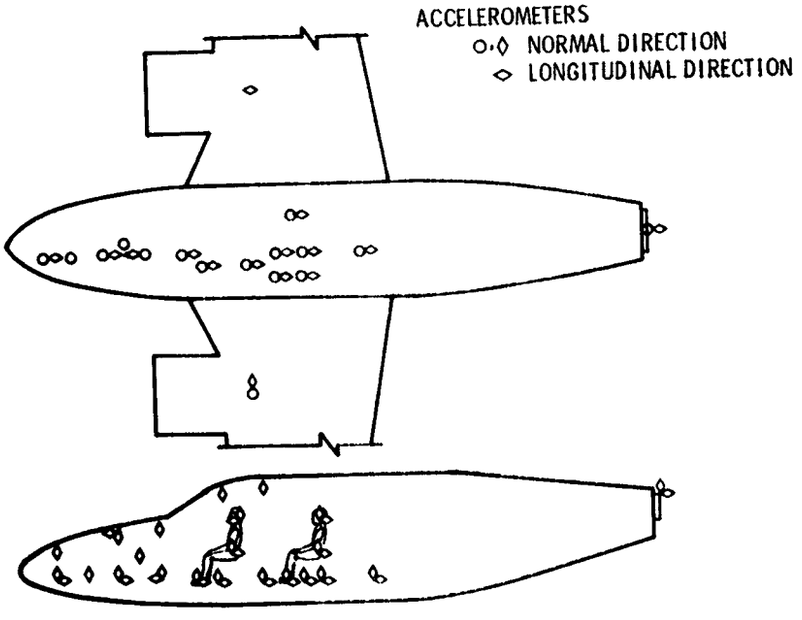

Figure 6.- Accelerometer layout for a symmetric crash test (no yaw).

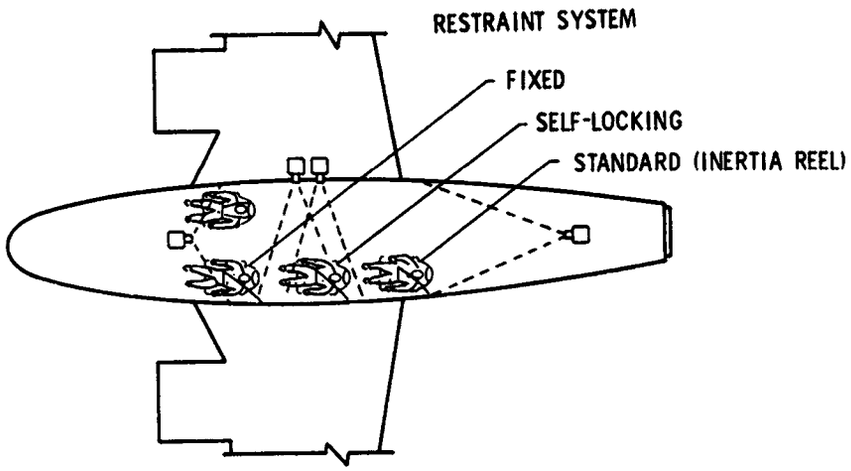

Figure 7.- Schematic of typical onboard camera and restraint-system arrangement.

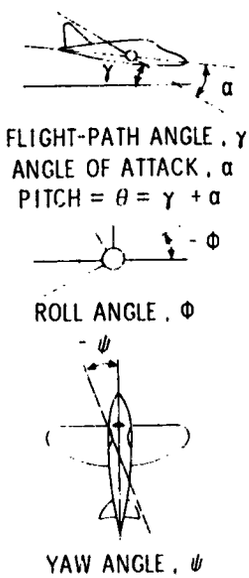

	PITCH, θ, deg				
VELOCITY =	13.4 m/sec (30 mph)	26.8 m/sec (60 mph)	26.8 * m/sec (60 mph)	40.2 m/sec (90 mph)	40.2 * m/sec (90 mph)
$\gamma = -5^0$				0	
$\gamma = -15^0$	-15	-15	-15 / -15	-15 -15	
		0		0	0
		15			
$\gamma = -30^0$		-30		-30	
		-15			
		0			
$\gamma = -45^0$		-45			
$\gamma = -15^0$ $\Phi = -15^0$		-15			
$\gamma = -15^0$ $\Phi = -30^0$		-15			

* LANDING GEAR DOWN

Figure 8.- Twin-engine crash test matrix. Shaded portion indicates completed tests.

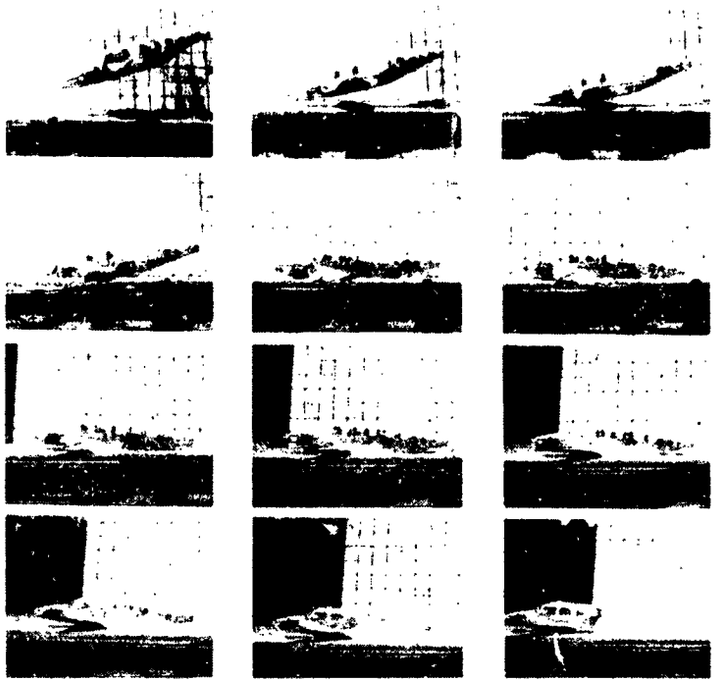

Figure 9.- Sequence of photographs taken during full-scale crash tests. 0.05 second between frames.

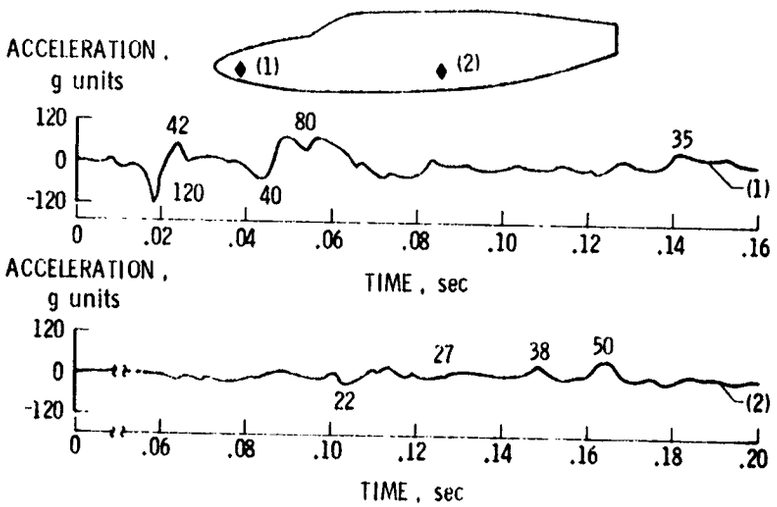

Figure 10.- Normal acceleration traces from two extreme points on floor beam.

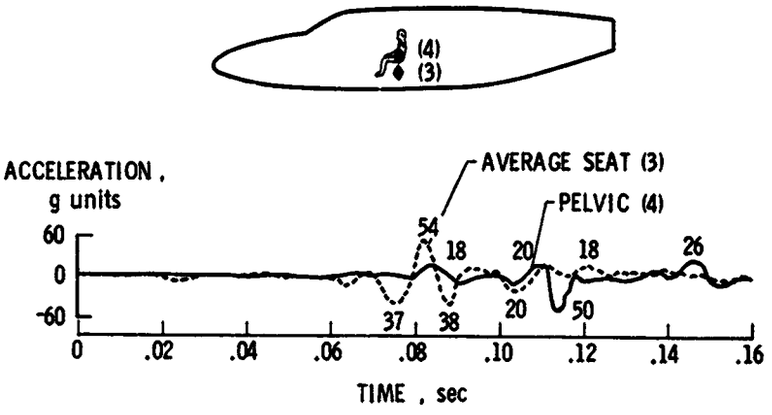

Figure 11.- Average normal acceleration at base of first passenger seat and at dummy's pelvis.

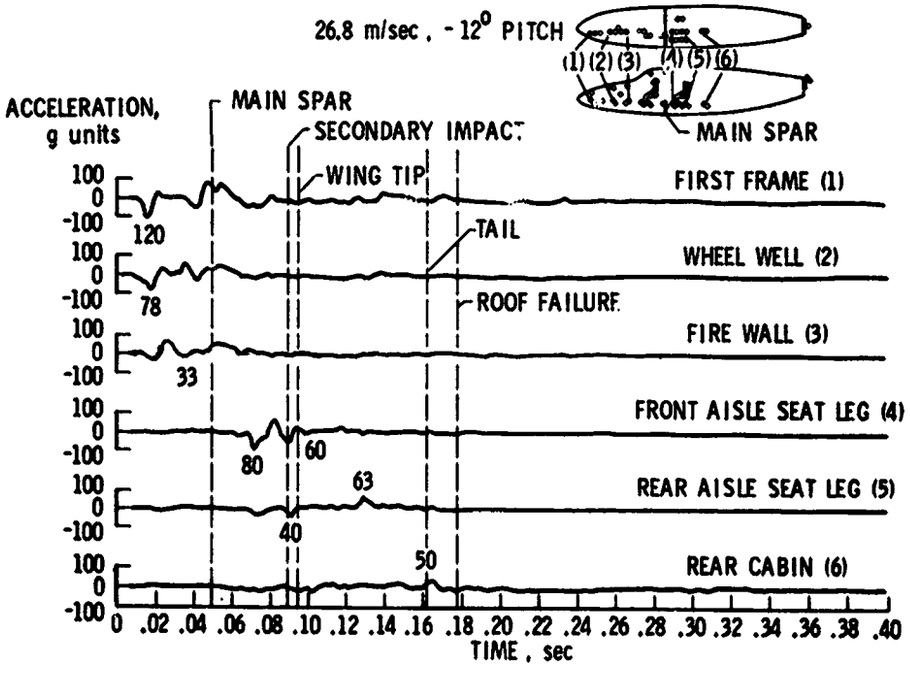

Figure 12.- Normal accelerations along fuselage floor beam.

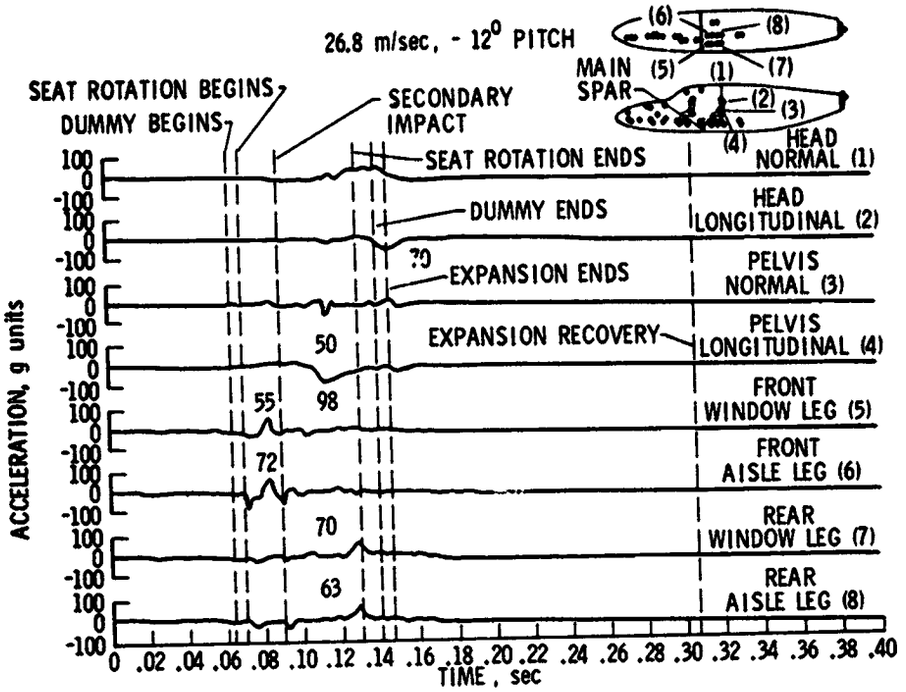

Figure 13.- Normal accelerations of first passenger seat and dummy.

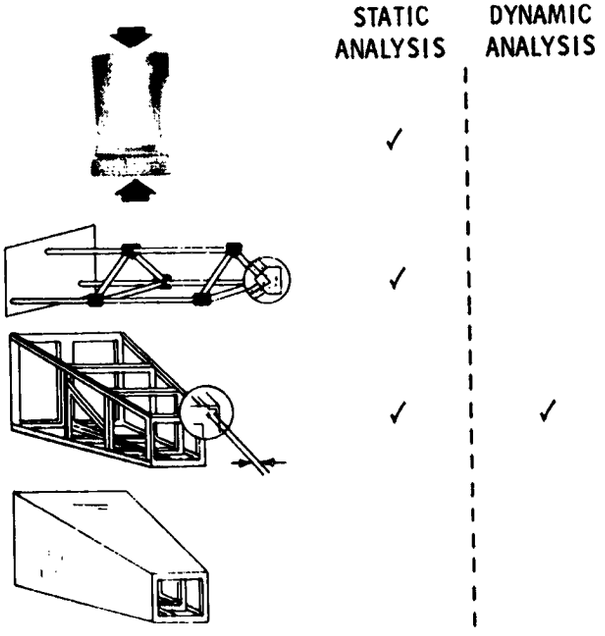

Figure 14.- Simplified structures used to corroborate experimental data with theoretical predictions.

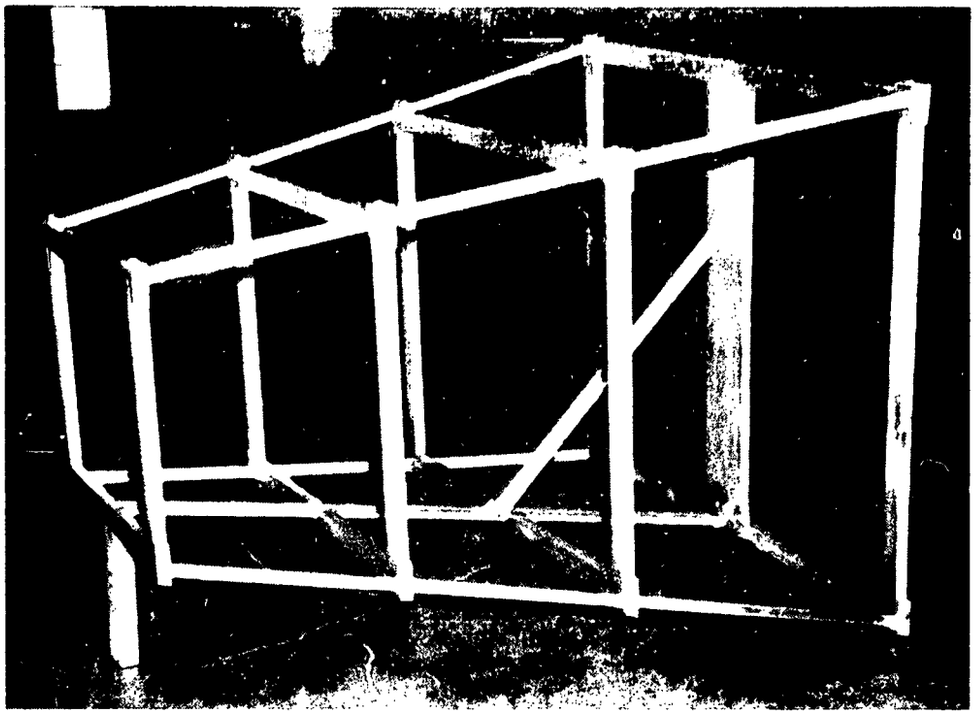

Figure 15.- Angular frame structure.

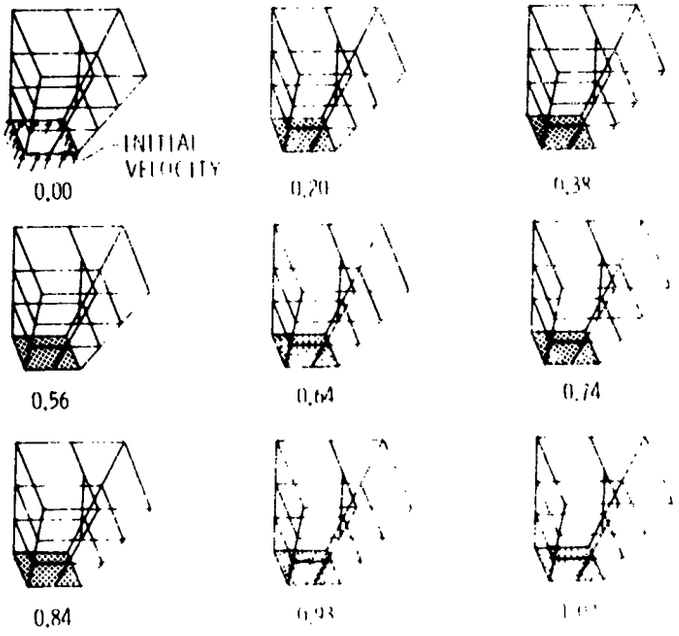

Figure 16.- Computer deformation patterns for angular frame loaded by initial velocity of [illegible].

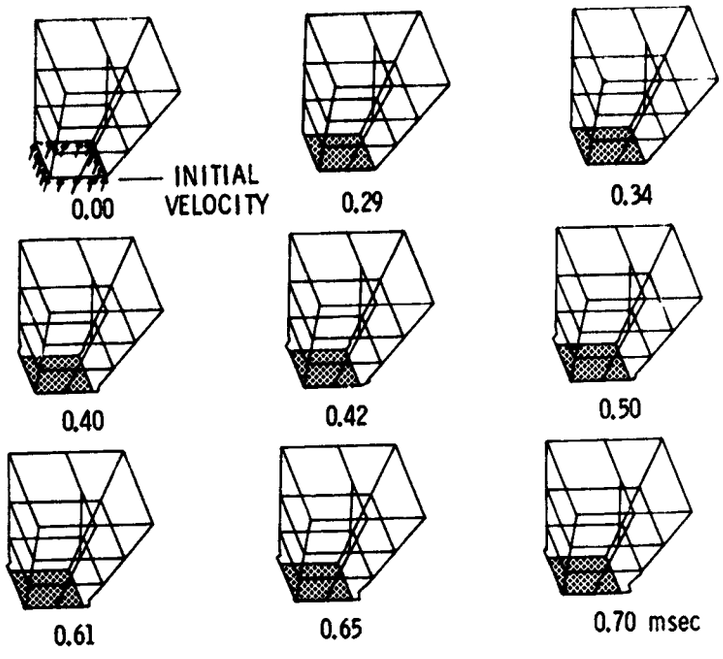

Figure 17.- Computer deformation patterns for angular frame loaded impulsively with initial velocity of 89.4 m/s (200 mph).

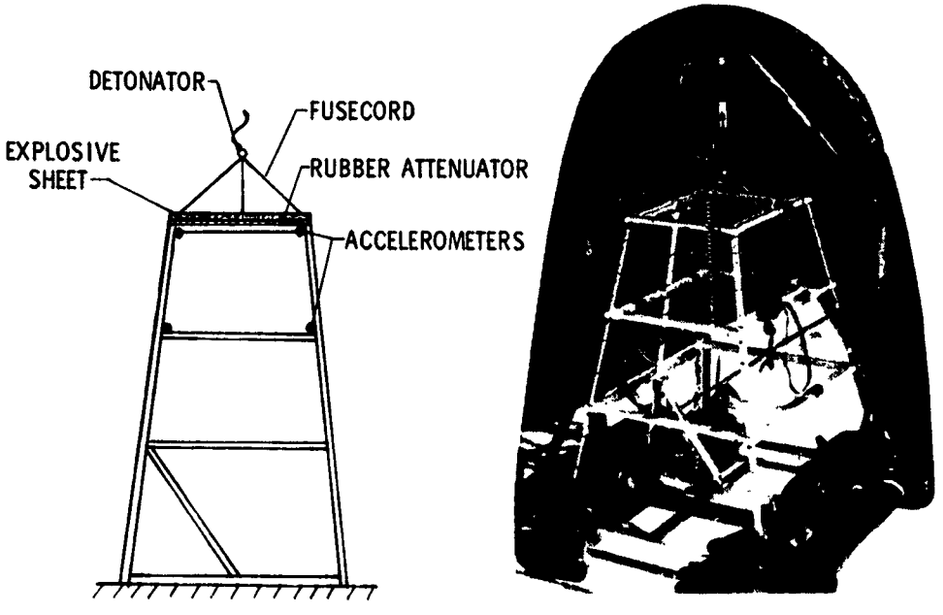

Figure 18.- Dynamic angular frame test setup.

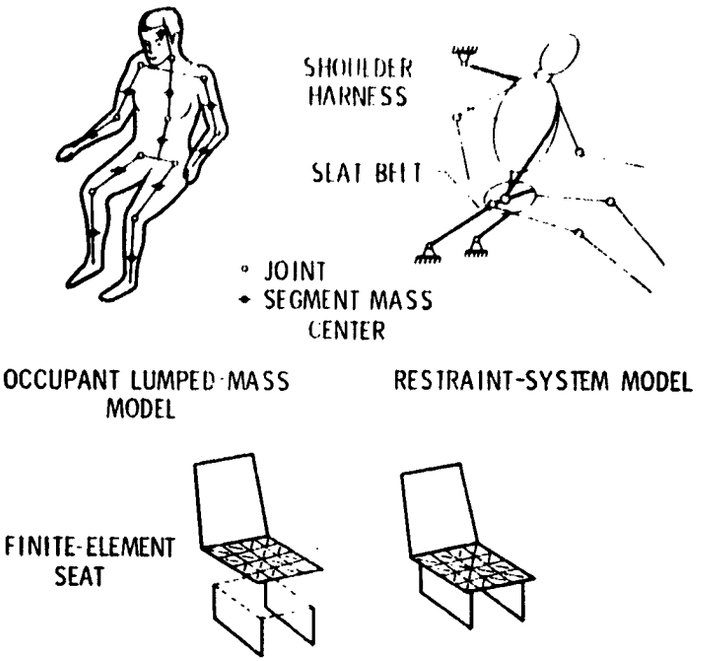

Figure 19.- Schematic of three-dimensional seat and occupant model.

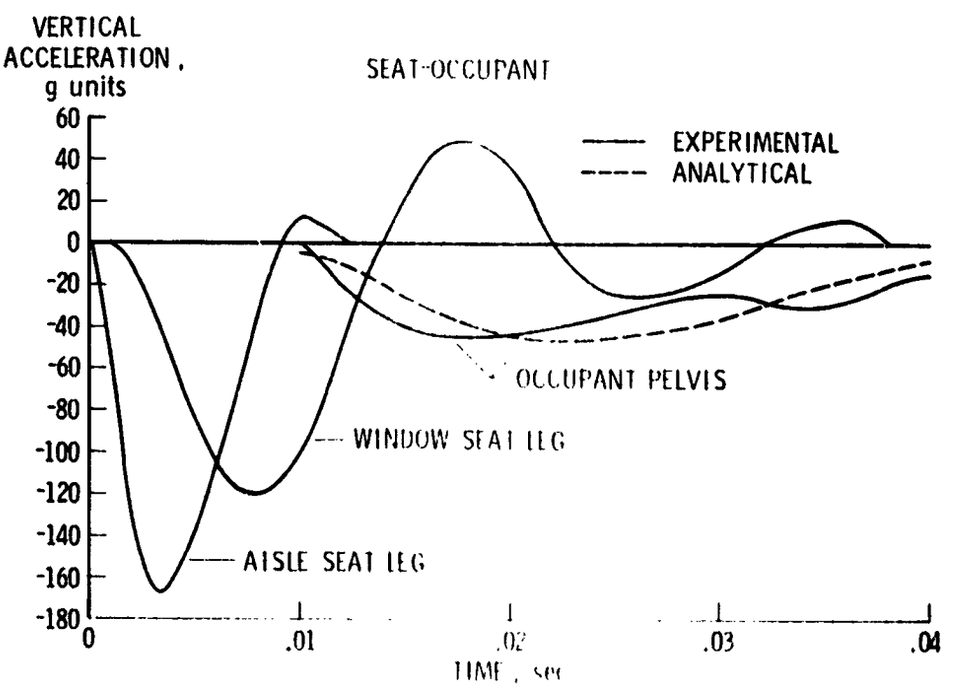

Figure 20.- Experimental data and computer predictions from aircraft section drop test.

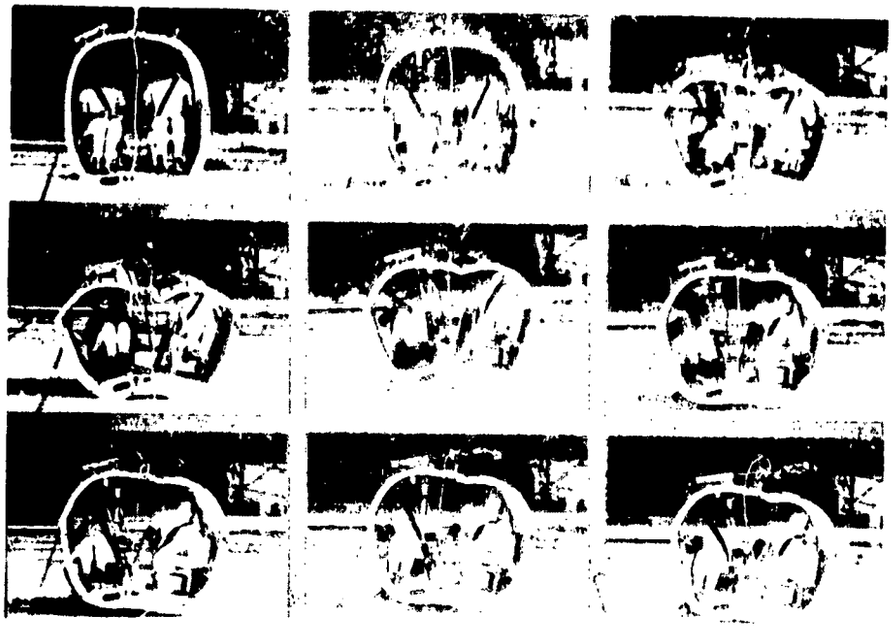

Figure 21.- Sequence of photographs taken during aircraft drop test. 0.05 second between frames.

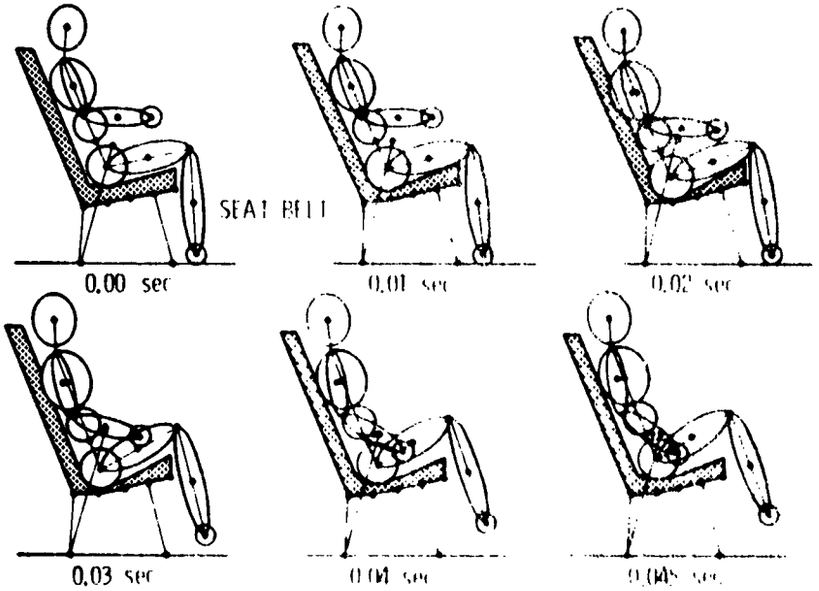

Figure 22.- Two dimensional computer graphic display of seat, occupant, and restraint system response for aircraft section drop test.